remote sensing

MDPI

Article

Retrieving Leaf Chlorophyll Content by Incorporating Variable Leaf Surface Reflectance in the PROSPECT Model

Feng Qiu [1], Jing M. Chen [1,2], Holly Croft [2], Jing Li [1], Qian Zhang [1], Yongqin Zhang [3] and Weimin Ju [1,*]

1 International Institute for Earth System Science, Nanjing University, Nanjing 210023, China
2 Department of Geography and Planning, University of Toronto, Toronto, ON M5S 3G3, Canada
3 Department of Biological Sciences, Delta State University, Cleveland, MS 38733, USA
* Correspondence: juweimin@nju.edu.cn

Received: 3 June 2019; Accepted: 1 July 2019; Published: 2 July 2019

Abstract: Leaf chlorophyll content plays a vital role in plant photosynthesis. The PROSPECT model has been widely used for retrieving leaf chlorophyll content from remote sensing data over various plant species. However, despite wide variations in leaf surface reflectance across different plant species and environmental conditions, leaf surface reflectance is assumed to be the same for different leaves in the PROSPECT model. This work extends the PROSPECT model by taking into account the variation of leaf surface reflection. In the modified model named PROSPECT-Rsurf, an additional surface layer with a variable refractive index is bounded on the N elementary layers. Leaf surface reflectance (Rs) is characterized by the difference between the refractive indices of leaf surface and interior layers. The specific absorption coefficients of the leaf total chlorophyll and carotenoids were recalibrated using a cross-calibration method and the refractive indices of leaf surface and interior layers were obtained during model inversion. Chlorophyll content (C_{ab}) retrieval and spectral reconstruction in the visible spectral region (VIS, 400–750 nm) were greatly improved using PROSPECT-Rsurf, especially for leaves covered by heavy wax or hard cuticles that lead to high surface reflectance. The root mean square error (RMSE) of chlorophyll estimates decreased from 11.1 μg/cm^2 to 8.9 μg/cm^2 and the Pearson's correlation coefficient (r) increased from 0.81 to 0.88 ($p < 0.01$) for broadleaf samples in validation, compared to PROSPECT-5. For needle leaves, r increased from 0.71 to 0.89 ($p < 0.01$), but systematic overestimation of C_{ab} was found due to the edge effects of needles. After incorporating the edge effects in PROSPECT-Rsurf, the overestimation of C_{ab} was alleviated and its estimation was improved for needle leaves. This study explores the influence of leaf surface reflectance on C_{ab} estimation at the leaf level. By coupling PROSPECT-Rsurf with canopy models, the influence of leaf surface reflectance on canopy reflectance and therefore canopy chlorophyll content retrieval can be investigated across different spatial and temporal scales.

Keywords: leaf chlorophyll content; leaf surface reflectance; leaf radiative transfer model; PROSPECT; hyperspectral remote sensing

1. Introduction

Leaf chlorophyll plays a critical role in plant photosynthesis and the conversion of CO_2 into stored carbohydrate. Accurate measurements of leaf chlorophyll content over different spatial and temporal extents using remote sensing techniques are needed for monitoring vegetation stress and productivity, and for forest management and precision agriculture applications. As light directly reflected from leaf epidermis does not interact with interior materials, it contains little information

on the leaf biochemistry and therefore should be excluded from the remotely sensed leaf reflectance. In the visible spectrum (VIS, 400–750 nm), about 3% to 10% (or higher for some species) of the light striking a leaf surface is directly reflected [1,2], accounting for up to 75% of the total reflected signal in the blue and red bands where light is strongly absorbed by pigments, and up to 25% of the total reflectance in the near infrared spectral region (NIR, 750–1300 nm) [3]. As a result, variations in leaf surface reflectance will introduce uncertainty to the deviation of leaf pigments from reflectance data across a wide range of species and plant functional types [4,5].

Leaf surface reflectance varies greatly with plant species, leaf development and environmental conditions [6–8]. It is controlled by epidermal characteristics such as the morphology and density of epicuticular waxes or trichomes [4,9], which can greatly enhance the leaf reflectance in the VIS [10,11]. Waxes also greatly increase the leaf reflectance in the NIR, whilst the effect of trichomes on NIR reflectance can be variable [4]. The magnitude and angular distribution of surface reflectance are dependent on the leaf surface biophysical properties. The highly absorbing visible wavelengths show a strong specular reflection compared to the more diffuse transmitted light [12]. Leaf specular reflectance from a surface is usually considered as wavelength-independent [13], as the leaf cuticle usually contains no pigments [7].

Polarization measurements are classically used to separate leaf surface specular reflectance (polarized) from interior diffuse reflectance (non-polarized) and obtain the optical properties of the leaf epidermis [14]. Leaf bidirectional reflectance measurements are also widely used to differentiate specular and diffuse components and to non-destructively estimate the roughness or refractive index of the epidermis [1,2]. However, these methods are complex and usually need specialized instruments that is not commonly used, precluding widespread measurement for model validation, and are hard to apply at the canopy scale.

Alternatively, efforts have been made to diminish leaf surface reflectance effects on the leaf chlorophyll content retrieval from remote sensing data. Leaf chlorophyll content estimation methods can be categorized into (1) parametric regression, (2) non-parametric regression, (3) physically based, and (4) hybrid methods (reviewed in [15]). Spectral indices, one of the most widely used parametric regression methods, have been modified to use reflectance in the blue wavelengths (~450 nm) to reduce the effects of surface reflectance on leaf pigment retrieval across different species [5]. Derivative spectra have also been found to be relatively insensitive to variations of leaf surface reflectance, especially using red-edge wavelengths [4,16]. However, regression methods suffer in terms of their transferability across temporal and spatial scales [17].

In comparison with regression methods, physically based models are underpinned by scientific theory and therefore have the ability to produce accurate and robust prediction of pigment content across different species and spatial scales. Bousquet et al. [2] proposed a three-parameter model differentiating surface reflectance from bidirectional measurements and retrieved values of cuticle refractive index and roughness parameter for the studied three species, but the model is over-parameterized and impractical for the commonly used leaf directional-hemispherical spectra. The PROSPECT model [18] is the most popular leaf radiative transfer model, due to its widespread validation and ease of inversion [19–21]. In PROSPECT, leaf surface reflectance is calculated from the refractive index of the leaf and the maximum incident angle, both of which are fixed values [18]. However, high surface reflectance due to heavy waxes on eucalypts leaves has shown to be a key source of uncertainty in pigment estimation from PROSPECT [22–24]. Jay et al. [13] proposed a physical model coupled with PROSPECT (PROCOSINE) to account for leaf surface reflectance and leaf orientation effects on leaf bidirectional reflectance factor (BRF), and successfully applied the model to close range hyperspectral images for retrieving foliar biochemistry. Li et al. [25] optimized the inversion strategies of PROSPECT for alleviating leaf surface reflectance effect, by introducing wavelet coefficient spectra generated after continuous wavelet transform (CWT) in the cost function, and improved the performance for foliar pigments retrieval using BRF spectra. Gerber et al. [26] used an additional layer in PROSPECT to compensate for the surface effects with a refractive index that is different from that of the leaf

interior. Nevertheless, it is assumed that the surface layer reflectance does not vary with different leaf samples, despite observations of large variations in leaf surface reflectance across species, growth stages, and environmental conditions [7,27].

In this study, we aim at extending PROSPECT-5 to consider variable leaf surface reflectance and alleviate its effect on leaf chlorophyll content estimation from hyperspectral leaf reflectance data. The objectives of this study are to: (1) introduce an additional surface layer bounded on the *N* elementary layers in PROSPECT-5, characterized by variable surface refractive index; (2) determine leaf surface and interior refractive indices for each samples and recalibrate the specific absorption coefficients for leaf total chlorophyll and carotenoids; and (3) evaluate the performance and sensitivity of chlorophyll content retrieval and leaf spectra reconstruction.

2. Data

2.1. Datasets

Seven independent datasets are used in this study. The datasets are fresh leaf samples collected and measured by different research groups (Table 1). The ANGERS dataset is downloaded online, shared by its authors. The other six datasets are from our field experiments in China (XS, BM, JTL, and NX) and Canada (Crop_UT and Needle_Zh). There are 922 fresh leaf samples from 56 species in total, including broadleaf and needle, dicotyledon and monocotyledon, trees and herbaceous, and annual and perennial plants, encompassing a wide range of physiological statuses. ANGERS has been widely used for model calibration, as it contains a large number of leaves from different species and a wide range of pigment contents [28]. ANGERS and one-fifth of the leaves in XS, BM, JTL, and NX datasets comprise the calibration dataset, and the rest samples are used as validation data.

Table 1. Main characteristics of the seven datasets used in this study.

	ANGERS	XS	BM	JTL	NX	Crop_UT	Needle_Zh
Year	2003	2014	2015	2015	2014	2013	2003–2004
Number of samples	276	175	54	35	140	152	90
Number of species	43	2 [a]	8 [b]	1 [c]	1 [d]	2 [e]	1 [f]
Spectral measurement devices	ASD FieldSpec Integrating sphere (IS)	ASD FieldSpec 3 ASD RTS-3ZC IS				ASD FieldSpec Pro FR Li-COR 1800 IS	ASD FieldSpec Pro FR Li-COR 1800 IS
Spectral sampling	1.4 nm (400–1000 nm), 2 nm (1000–2500 nm)						
Solvent for pigments	Ethanol 95%	Acetone 100%				DMF *	DMF
Method for pigments	[29]	[29]				[30]	[31]
Chlorophyll (μg/cm^2)							
Max	106.7	93.8	80.8	83.9	71.7	92.5	62.6
Min	0.8	16.8	1.4	30.1	20.1	0.4	12.0
Mean	33.9	50.9	40.1	56.1	44.0	43.6	29.3
SD **	21.7	15.5	15.5	15.9	11.2	20.3	9.1
Carotenoids (μg/cm^2)							
Max	25.3	17.2	16.7	15.2	12.8	\	10.3
Min	0.0	3.8	4.4	6.8	3.9	\	3.2
Mean	8.7	9.9	9.9	10.7	8.0	\	6.3
SD	5.1	2.9	2.7	2.3	1.9	\	1.6
Water (g/m^2)						\	
Max	340.0	144.8	206.1	312.0	168.8	\	\
Min	43.9	59.0	65.0	143.8	84.4	\	\
Mean	116.2	102.9	115.3	213.6	117.2	\	\
SD	48.6	15.9	29.1	47.0	16.1	\	\
Dry matter (g/m^2)						\	
Max	331.0	166.2	145.6	185.9	56.1	\	\
Min	16.6	55.4	49.0	67.0	8.7	\	\
Mean	52.4	100.9	81.8	122.6	33.2	\	\
SD	36.7	24.7	21.8	26.9	6.0	\	\

[a] Species including *Liquidambar formosana L. and Quercus acutissima L.*; [b] Species including *Koelreuteria paniculata L., Sapium sebiferum L., Malus spectabilis L., Lagerstroemia indica L., Cerasus serrulata L., Liquidambar formosana L., Populus nigra L.*, and *Cyclocarya paliurus L.*; [c] *Ligustrum lucidum L.*; [d] *Zea mays L.*; [e] *Zea mays L.* and *Triticum aestivum L.*; [f] *Picea mariana* (Mill.). * Dimethylformamide. ** Standard Deviation

2.2. Leaf Spectral Measurements

In the experiments for the seven datasets, leaf samples were transported to a laboratory for spectral measurements immediately after leaf sampling. Leaf directional-hemispherical spectra (<2 nm step over 400–2500 nm) for the upper surface of the leaf samples were measured using a field spectroradiometer coupled with an integrating sphere (Table 1). For needle optical measurements in Needle_Zh, a special carrier was used to hold the needles and to present them to the port of the integrating sphere [32,33]. These measurements include both leaf total reflectance and transmittance but does not discriminate between leaf surface and interior reflectance. The spectra in the ANGERS dataset shared online were already smoothed and processed to 1 nm interval. The measured spectra in the other six datasets were resampled to 1 nm interval and smoothed using the Savizky–Golay approach with a third-order polynomial function using 25 nm bandwidth [34].

2.3. Leaf Biochemical Constituent Determination by Destructive Sampling

Four leaf biochemical constituents were measured, including leaf total chlorophyll (C_{ab}, sum of chlorophyll a and b), total carotenoids (C_{xc}), water (*EWT* for equivalent water thickness), and dry matter (*LMA* for leaf mass per area). Right after the leaf spectral measurements, leaf disks were sampled from the same leaf where spectral measurements took place. A cork-borer of known area was used to punch out several leaf disks from the same leaf, avoiding main leaf veins if possible. The sampled needles were scanned on a flatbed scanner for the total projected area. Then the sampled leaf disks or needles were separated into two groups, one for water and dry matter measurements and the other for pigment determination after being frozen.

First, the total fresh weight of one group of disks (*Fw*, in g) was measured and then dried in an oven at 65 °C for at least 48 h and reweighed until there was little change in the dry weight (*Dw*, in g). The *EWT* and *LMA* was determined as: *EWT* (in g/m^2) = (*Fw*−*Dw*)/area of disks and *LMA* (in g/m^2) = *Dw*/area of disks. The other group of the disks were frozen after sampling, ground or placed in the organic solvents (ethanol, acetone, or dimethylformamide (DMF)) in the dark, until the pigments were fully extracted. After centrifugation, the extracted solution was diluted with the corresponding solvent to a certain volume. The absorbance of the solution was measured using UV–VIS spectrophotometers (UV1800, SHIMADZU Corporation, Japan) and converted to pigment content using specific calibration coefficients for different solvents provided by [29,35,36].

3. Methods

3.1. Addition of a Surface Layer with a Variable Refractive Index

The PROSPECT model simulates leaf directional-hemispherical reflectance and transmittance (400–2500 nm) according to input leaf biochemical contents (C_{ab}, C_{xc}, *EWT*, *LMA*, etc.) and a structure parameter *N* [18,24,28]. It is based on the plate model [37] that treats a leaf as a stack of *N* homogeneous elementary layers characterized by an absorption coefficient and a refractive index. When a beam is incident on the boundary of a plate, the transmissivity (t_α) and reflectivity (r_α) of the surface depend on the effective refractive index (n) and the maximum incidence angle (α) defining the solid angle of the incident beam:

$$t_a = \mathrm{tav}(\alpha, n) \quad (1)$$

$$r_a = 1 - t_a \quad (2)$$

where tav is the transmissivity of the surface of the top plate.

Due to the undulating shape of the surface of the leaves, the maximum incidence angle for the top layer (α_{surf}) is different from interior layers ($\alpha_{\mathrm{in}} = 90°$) where the light stream is assumed to be isotropic. The value of α_{surf} is set to the optimum value 59° in the early versions of PROSPECT and reset to 40° in the versions after PROSPECT-4. The surface effects on leaf optical properties are simplified by using α_{surf} in all existing versions of the PROSPECT model. Since α_{surf} is constant and the refractive index

(n) is a unique spectrum for all leaves and is identical for the N layers, the surface effects in PROSPECT does not change with leaf samples. The mean reflectance of the upper boundary layer from 400–800 nm (r_a) is 0.037. However, leaf surface reflectance could vary greatly with plant species, leaf development, and environmental conditions [6–8]. Gerber et al. [26] added an additional non-absorbing surface layer on top of the N elementary layers in PROSPECT to compensate for the surface effects. The refractive index of the surface layer (n_{surf} (λ)) is different from that of the interior elementary layers (n_{in} (λ)), and their difference determines the surface reflectance as Fresnel coefficients depend on the effective refractive index of the interface. Nevertheless, since n_{surf} (λ) and n_{in} (λ) in their study were fixed spectra, the surface reflectance did not change with the leaf samples.

Therefore, we add a non-absorbing surface layer similar to that of Gerber et al. [26] in PROSPECT-5, but with variable refractive indices for surface and interior layers. The surface layer is bound to the first of the N elementary layers without any interspace filled by air. According to Gerber et al. [26], this additional surface layer can be considered as an equivalent layer compensating surface effects rather than a true representation of leaf cuticle. Figure 1 shows the basic structure of the modified model (denoted as PROSPECT-Rsurf).

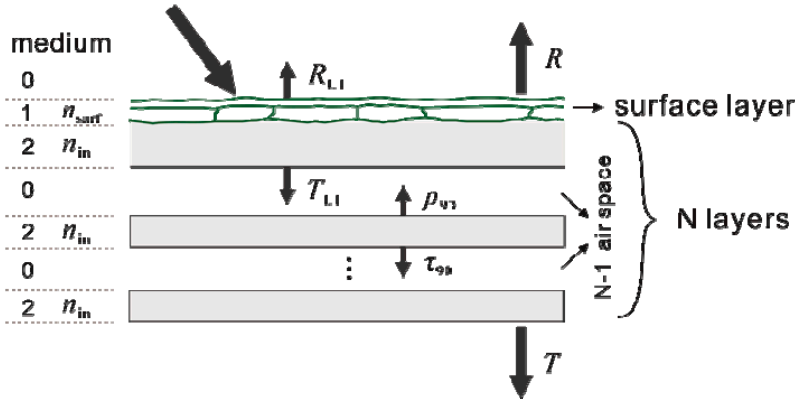

Figure 1. Structure of the PROSPECT-Rsurf model. The medium 0, 1, 2 refer to air, surface (refractive index n_{surf}), and leaf interior (n_{in}), respectively.

When light incidents on top of the surface layer, the maximum incidence angle (α_{surf}) is assumed to be 40° and becomes isotropic after transmission through this layer, following the principles in PROSPECT-5 [28]. The reflectance (R_{L1}) and transmittance (T_{L1}) of the first elementary layer coated with the surface layer are calculated as,

$$R_{L1} = r_{01} + \frac{t_{01} \cdot t_{10} \cdot r_{120}}{1 - r_{10} \cdot r_{120}} \quad (3)$$

$$T_{L1} = \frac{t_{01} \cdot t_{120}}{1 - r_{10} \cdot r_{120}} \quad (4)$$

$$\text{with } r_{120} = r_{12} + \frac{t_{12} \cdot t_{21} \cdot r_{20} \cdot \theta^2}{1 - r_{20} \cdot r_{21} \cdot \theta^2} \quad (5)$$

$$\text{and } t_{120} = \frac{t_{12} \cdot t_{20} \cdot \theta}{1 - r_{20} \cdot r_{21} \cdot \theta^2} \quad (6)$$

where the subscript 0 corresponds to the air, 1 to the surface layer, and 2 to the leaf interior; r_{120} and t_{120} are reflectance and transmittance when light emerges from the surface layer and passes through the first elementary layer; θ is the transmission coefficient of the elementary layer; and r_{ij} and t_{ij} (i, j = 0, 1, 2) are

the reflectivity and transmissivity at the interface when light emerges from medium i into j, respectively, defined by the maximum incident angle (α) and effective refractive index (n') as:

$$t_{ij} = \text{tav}(\alpha, n') \tag{7}$$

$$r_{ij} = 1 - t_{ij} \tag{8}$$

where $n' = n_j/n_i$. The reflectance ρ_{90} and transmittance τ_{90} of the other N-1 elementary layer follow Equations (1) to (6) in [18]. The total reflectance (R) and transmittance (T) of a leaf is calculated by stacking the first layer group (a plate coated with surface layer) and the N-1 layers according to [18].

Leaf surface reflectance is specified by the multiple scattering between the surface layer and the first elementary layer, characterized by the two refractive indices n_{surf} (λ) and n_{in} (λ). Reflectance of the additional surface layer (Rs) is defined based on the calculation of the reflectance of the first group layer (R_{L1}) using Equations (3) to (8), by assuming the transmittance of the first elementary layer (θ) to be 0:

$$Rs = r_{01} + \frac{t_{01} \cdot t_{10} \cdot r_{12}}{1 - r_{10} \cdot r_{12}} \tag{9}$$

The transmittance of the surface layer is:

$$Ts = 1 - Rs \tag{10}$$

Based on the definition, the surface layer reflectance in PROSPECT-Rsurf is the surface directional-hemispherical reflectance, consistent with leaf reflectance and transmittance simulated in the model. It is the integration of leaf surface reflectance over the hemisphere from the leaf upper surface which includes the leaf specular reflectance as well as multiple scattering between the surface and interior layers.

The surface refractive index n_{surf}(λ) changes with different epidermal materials with various morphology and density, while n_{in}(λ) is determined by the internal structure and the organization and composition of internal leaf tissues and air spaces. According to Kramers–Kronig (K–K) relations [38], the real (refractive index) and imaginary (absorption coefficient) part of the complex refractive index are physically linked. Chen and Weng [39] used the K–K relations to derive the effective refractive index with promising results and demonstrated variations of the leaf refractive index for different leaf samples. They found that the leaf refractive index decreases almost monotonically with the wavelength (400–2500 nm), confirming the refractive index spectrum used in PROSPECT-3 (n_{P3}(λ)). However, since the K–K relations require complete electromagnetic spectrum of the biochemical absorption coefficient which are difficult to obtain so far, it is impracticable for most of the commonly used leaf spectral databases covering a limited range of the spectrum [24]. In the latest version PROSPECT-D, n_{P3}(λ) is adopted instead of the one used in PROSPECT-5 in order to avoid artifacts resulting from numerical optimization [24]. Since direct measurements of the leaf surface and internal refractive indices are difficult and the variation of the leaf tissue refractive index with wavelengths remains unclear, the following two assumptions are made in this study, (1) the spectral variation patterns of n_{surf}(λ) and n_{in}(λ) follow the pattern of n_{P3}(λ); and (2) n_{surf}(λ) is higher than n_{in}(λ). The two refractive indices n_{surf} (λ) and n_{in}(λ) are defined by

$$n_{surf}(\lambda) = f_{surf} \cdot n_{P3}(\lambda) \tag{11}$$

$$n_{in}(\lambda) = f_{in} \cdot n_{P3}(\lambda) \tag{12}$$

where f_{surf} and f_{in} are fractions of the surface and interior refractive indices, respectively, which are independent of wavelengths but vary with leaf samples. In this way, we can focus on the variations of the surface and interior refractive indices between different leaves using only two parameters for each

sample, while the spectral variation characteristics of the two refractive indices are unaltered. In order to keep n_{surf} (λ) higher than n_{in}(λ) in the model, n_{surf} (λ) is expressed as

$$n_{\text{surf}}(\lambda) = f'_{\text{surf}} \cdot n_{\text{in}}(\lambda) \tag{13}$$

with f'_{surf} higher than 1. The factor f'_{surf} is the relative refractive index between the leaf surface and the interior. Therefore, we have two variables f'_{surf} and f_{in} in addition to the structure parameter N and biochemical contents (C_{ab}, C_{xc}, EWT, and LMA) in PROSPECT-Rsurf. The main symbols used in this study and their meanings are listed in Table A1. Considering that leaf pigments absorb light in the VIS domain and effects of the leaf surface reflectance on leaf spectra are significant in the VIS, we make the above modifications in PROSPECT-Rsurf in the range from 400 to 800 nm in this study.

3.2. Model Calibration

After adding the new surface layer and the two refractive indices in PROSPECT-Rsurf, the specific absorption coefficient (SAC) of leaf constituents can be recalibrated from wavelength to wavelength. Since absorption by leaf dry matter and water is low in the VIS, only the SAC of total chlorophyll (k_{Cab}(λ)) and carotenoids (k_{Cxc}(λ)) are recalibrated. The structure parameter N and the refractive index fractions f'_{surf} and f_{in} change from leaf to leaf and are assumed to be wavelength independent. Since N, f'_{surf}, and f_{in} cannot be directly measured, they are determined in the recalibration process. In order to avoid unfeasibly large computation introduced by concurrently optimizing all the parameters (N, f'_{surf}, f_{in}, k_{Cab}(λ), and k_{Cxc}(λ) at each wavelength λ from 400–800 nm), the recalibration process is split into two steps. First, the wavelength-independent N, f'_{surf}, and f_{in} are determined, and then k_{Cab}(λ) and k_{Cxc}(λ) are determined wavelength by wavelength. Due to the possible interaction between the two steps, we performed a cross calibration iteratively until the optimized values of these parameters remain almost unchanged. Detailed descriptions are as follows.

3.2.1. Determination of N, f'_{surf} and f_{in}

The variables N, f'_{surf}, and f_{in} are estimated for each leaf individually from the measured spectra (400–800 nm) with measured C_{ab}, C_{xc}, EWT, and LMA as input through a numerical optimization process, by finding the best combination of variables that minimizes the merit function:

$$\begin{aligned} J\left(N, f'_{surf}, f_{in}\right) = \sum_{\lambda=400}^{800} \Bigg[& \left(R_{\text{meas},\lambda} - R_{\text{mod},\lambda}\left(N, C_{ab}, C_{xc}, EWT, LMA, f'_{surf}, f_{in}\right)\right)^2 \\ & + \left(T_{\text{meas},\lambda} - T_{\text{mod},\lambda}\left(N, C_{ab}, C_{xc}, EWT, LMA, f'_{surf}, f_{in}\right)\right)^2 \Bigg] \end{aligned} \tag{14}$$

where $R_{\text{meas},\lambda}$ and $T_{\text{meas},\lambda}$ are the measured leaf total reflectance and transmittance at wavelength λ, respectively, and $R_{\text{mod},\lambda}$ and $T_{\text{mod},\lambda}$ are simulated by PROSPECT-Rsurf. The bound-constrained optimization package FMINSEARCHBND.M [40] in the Matlab software is used. The initial values of N, f'_{surf}, and f_{in} are 1.5 (1–5), 1.1 (1.0001–3), and 1 (0.7–3), respectively, with constrained values given in brackets. The ranges of f'_{surf} and f_{in} are set according to the measurements and simulation of the leaf refractive index in previous studies in [1,2,26,39,41].

3.2.2. Adjustment of the Specific Absorption Coefficients

After determining N, f'_{surf}, and f_{in}, the SAC of total chlorophyll and carotenoids are adjusted through optimization using all leaves comprising the calibration dataset. Similar to the process described in [28], the SAC values of chlorophyll ($k_{Cab,\lambda}$) and carotenoids ($k_{Cxc,\lambda}$) at each wavelength are obtained by minimizing the merit function:

$$J\left(k_{Cab,\lambda}, k_{Cxc,\lambda}\right) = \sum_{i=1}^{m} \left(R^i_{\text{meas},\lambda} - R^i_{\text{mod},\lambda}\left(k^i_\lambda\right)\right)^2 + \left(T^i_{\text{meas},\lambda} - T^i_{\text{mod},\lambda}\left(k^i_\lambda\right)\right)^2 \tag{15}$$

where m is the total sample number, k_λ^i is the total absorption coefficient of the elementary layer at wavelength λ for sample i, which is calculated from the structure parameter N and the biochemical contents as follows:

$$k_\lambda^i = \frac{k_{Cab,\lambda} \cdot C_{ab}^i + k_{Cxc,\lambda} \cdot C_{xc}^i + k_{EWT,\lambda} \cdot EWT^i + k_{LMA,\lambda} \cdot LMA^i}{N_i} \tag{16}$$

where $k_{EWT,\lambda}$ and $k_{LMA,\lambda}$ are SAC of EWT and LMA in PROSPECT-5 at λ, respectively, N_i is the structure parameter of sample i; and ${C^i}_{ab}$, ${C^i}_{xc}$, EWT^i, and LMA^i are the measured four biochemical contents of sample i. The initial values of $k_{Cab,\lambda}$ and $k_{Cxc,\lambda}$ are 0.05 and 0.2, respectively. During the inversion, their values were limited in the range of 0–0.1 and 0–0.5, respectively.

3.2.3. Cross Calibration

After step (2), the adjusted SACs are used for recalculating the values of N, ${f'}_{\mathrm{surf}}$, and f_{in} (step (1)). Then the SAC values of C_{ab} and C_{xc} are re-adjusted (step (2)) and new sets of N, ${f'}_{\mathrm{surf}}$, and f_{in} can be subsequently determined (step (1)). We repeat steps (1) and (2) in this way for several times until the optimized N, ${f'}_{\mathrm{surf}}$, and f_{in} values for each sample and the $k_{Cab,\lambda}$ and $k_{Cxc,\lambda}$ spectra from 400 nm to 800 nm remain nearly unchanged (changes less 0.1%).

3.3. Model Validation: Criteria for the Comparison of Model Performance

We performed model inversions on the validation datasets separated into broadleaf and needle leaf samples with PROSPECT-5 and PROSPECT-Rsurf. The performances of the two models are compared in terms of Cab estimation and leaf spectral fit. PROSPECT-Rsurf is inverted on the validation datasets using the following merit function:

$$\begin{aligned} J\left(N, C_{ab}, C_{ar}, EWT, LMA, f\prime_{surf}, f_{in}\right) = \sum_{\lambda=400}^{800} \Big[& \left(R_{\mathrm{meas},\lambda} - R_{\mathrm{mod},\lambda}\left(N, C_{ab}, C_{ar}, EWT, LMA, f\prime_{surf}, f_{in}\right)\right)^2 \\ & + \left(T_{\mathrm{meas},\lambda} - T_{\mathrm{mod},\lambda}\left(N, C_{ab}, C_{ar}, EWT, LMA, f\prime_{surf}, f_{in}\right)\right)^2 \Big] \end{aligned} \tag{17}$$

where $R_{\mathrm{meas},\lambda}$ and $T_{\mathrm{meas},\lambda}$ are the measured leaf total reflectance and transmittance at wavelength λ, respectively, $R_{\mathrm{mod},\lambda}$ and $T_{\mathrm{mod},\lambda}$ are the ones simulated by PROSPECT-Rsurf.

Standard deviation (σ) and coefficient of variability (CV) are calculated to characterize the distribution of variables. Pearson's correlation coefficient (r), root mean square error (RMSE), and bias (BIAS) between the retrieved and measured variables are calculated to evaluate the differences between the measured and estimated variables (such as pigment content, leaf reflectance, or transmittance):

$$\mathrm{CV}(\%) = \frac{\sigma}{\overline{y}_j} \times 100 \tag{18}$$

$$\mathrm{RMSE} = \sqrt{\frac{\sum_{j=1}^{n}\left(y'_j - y_j\right)^2}{n}} \tag{19}$$

$$\mathrm{BIAS} = \frac{\sum_{j=1}^{n}\left(y'_j - y_j\right)}{n} \tag{20}$$

where y_j is the measurements, y_j their mean, y'_j the modeled values, and n the sample numbers.

3.4. Model Sensitivity

Since there are no direct measurements of leaf surface and interior refractive indices in this study, the uncertainty in determining ${f'}_{\mathrm{surf}}$ and f_{in} (corresponding to n_{surf} and n_{in}) from model inversion using the experimental data and the effect of such uncertainty on the quality of the calibration should be evaluated. We perform several steps of sensitivity analysis to understand the influence of noise in the

measured spectral data on surface and interior refractive indices determination, and their uncertainty on the adjustment of SACs and on the overall model performances.

3.4.1. Global Sensitivity Analysis

A global sensitivity analysis was set up to evaluate the contribution of the variability in each input variable (N, f'_{surf}, f_{in}, C_{ab}, C_{xc}, EWT, and LMA) to output reflectance or transmittance from PROSPECT-Rsurf. Sobol's sensitivity analysis was implemented using a Matlab software tool (GAST) [42]. A dataset of 5000 random parameters was generated using the data range in Table 2 according to measurements and model inversion results.

Table 2. Data range for Sobol sensitivity analysis.

Variable	Range of Sobol Set
N	1–3
f'_{surf}	1–1.1
f_{in}	0.76–1.15
C_{ab}	0–120 (μg/cm^2)
C_{xc}	0–3 (μg/cm^2)
EWT	40–345 (g/m^2)
LMA	17–330 (g/m^2)

3.4.2. Sensitivity of Model Calibration

We first investigate the sensitivity of N, f'_{surf}, and f_{in} estimation to noise in spectral measurements. Randomly generated Gaussian noises with standard deviation (σ) set to be 2% of the measured R or T (the mean value μ = 0) are added to measured R and T, respectively, at each wavelength from 400–800 nm. Then N, f'_{surf}, f_{in}, and biochemical parameters are derived from the calibrated PROSPECT-Rsurf model inversion following the procedure described in step (1) of Section 3.2. The operation is repeated 100 times for each sample in the validation datasets.

Second, randomly generated Gaussian noises (σ = 0.009 and 0.039, σ of f'_{surf} and f_{in} derived from inversion, respectively) are introduced to f'_{surf} and f_{in}, respectively, and the noisy datasets are used to determine $k_{Cab,\lambda}$ and $k_{Cxc,\lambda}$ following the method described in step (2) of Section 3.2 in order to investigate the uncertainty introduced by noise in f'_{surf} and f_{in} determination.

3.4.3. Sensitivity of Model Performance

In order to evaluate the influence of uncertainty in f'_{surf} and f_{in} estimation on leaf chlorophyll content retrieval, we add Gaussian noises (σ = 0.009 and 0.039) to f'_{surf} and f_{in} derived from inversion, respectively. Then the noisy f'_{surf} and f_{in} (denoted as $f'_{\mathrm{surf\text{-}noise}}$ and $f_{\mathrm{in\text{-}noise}}$) are used as input parameters when retrieving N and the biochemical parameters using the following merit function:

$$J(N, C_{ab}, C_{xc}, EWT, LMA) = \sum_{\lambda=400}^{800} \left(R_{\mathrm{meas},\lambda} - R_{\mathrm{mod},\lambda}\left(N, C_{ab}, C_{xc}, EWT, LMA, f'_{surf-\mathrm{noise}}, f_{in-\mathrm{noise}}\right)\right)^2 + \left(T_{\mathrm{meas},\lambda} - T_{\mathrm{mod},\lambda}\left(N, C_{ab}, C_{xc}, EWT, LMA, f'_{surf-\mathrm{noise}}, f_{in-\mathrm{noise}}\right)\right)^2 \quad (21)$$

where $R_{\mathrm{meas},\lambda}$ and $T_{\mathrm{meas},\lambda}$ are the measured leaf total reflectance and transmittance at wavelength λ, respectively, $R_{\mathrm{mod},\lambda}$ and $T_{\mathrm{mod},\lambda}$ are the ones simulated by PROSPECT-Rsurf. The retrieved groups of biochemical contents are compared with measurements to evaluate the performance of the model for both validation and calibration datasets.

4. Results

4.1. Validation of Model Performances

4.1.1. Recalibrated Specific Absorption Coefficients

Figure 2 displays the SACs of total chlorophyll ($k_{Cab,\lambda}$) and carotenoids ($k_{Cxc,\lambda}$) in PROSPECT-Rsurf (P-Rs) and PROSPECT-5 (P-5). The differences between the two models are subtle, with a little higher difference between 500 and 550 nm. In P-Rs between 500 and 550 nm, $k_{Cab,\lambda}$ is slightly higher and k_{Cxc} is slightly lower than those in P-5. Considering the variation of leaf surface reflection does not introduce large changes in the SACs of pigments.

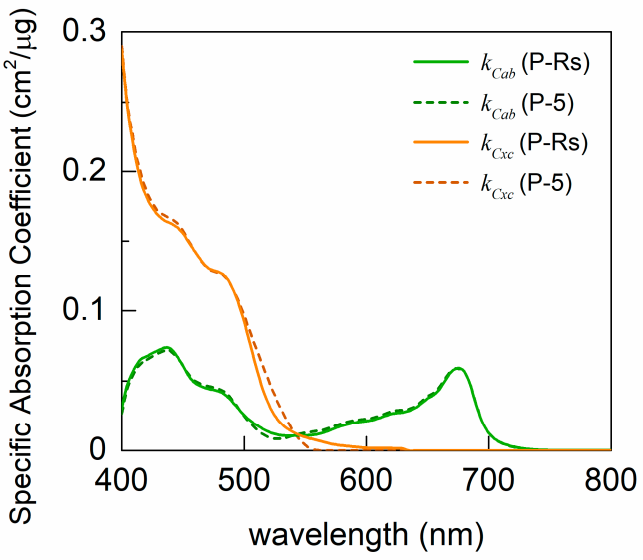

Figure 2. Specific absorption coefficients (SAC) of total chlorophyll (k_{Cab}, green lines) and carotenoids (k_{Cxc}, orange lines). The solid lines are from PROSPECT-Rsurf (P-Rs), and the dashed lines from PROSPECT-5 (P-5).

4.1.2. Chlorophyll Content Estimation

Figure 3 compares the performances of chlorophyll content estimation for PROSPECT-Rsurf (P-Rs) to PROSPECT-5 (P-5). The color of the points in Figure 3 corresponds to the surface layer reflectance (*Rs*). The results are demonstrated in three groups: the calibration, broadleaf samples in validation, and needle leaves in validation datasets. Estimation of C_{ab} using P-Rs is improved for the broad leaves in validation datasets (Figure 3b), with RMSE decreasing from 11.12 to 8.87 μg/cm^2, r increasing from 0.81 to 0.88, and BIAS adjusted from −3.31 to 0.65. For some of the broadleaf validation samples with high *Rs*, the underestimation of C_{ab} using P-5 due to the underestimation of *Rs* is alleviated in P-Rs with BIAS close to 0 (0.65). Furthermore, the overestimation of extremely low C_{ab} samples is corrected.

For needle leaves, the C_{ab} estimated using P-Rs is highly correlated with the measurements (r = 0.89), and much higher than those from P-5 (r = 0.72). However, C_{ab} estimated using P-Rs is systematically overestimated, resulting in high RMSE and BIAS compared to those using P-5 (Figure 3c,d). According to [33], the main reason for the overestimation is that the assumption in the PROSPECT model that a leaf is horizontally infinite may not hold for needle leaves since the needle width is comparable to the needle thickness. The amount of light that escapes from needle edge could be large, leading to the overestimation of leaf reflectance (R) and transmittance (T) using both P-Rs and P-5. Consequently, the overestimation of leaf R and T in VIS leads to increases in C_{ab} in order to lower R and T to fit measured spectra during P-Rs model inversion. However, the overestimation of C_{ab} using P-5 is minor, since the abovementioned overestimation of R and T caused by needle edge effects is partially offset by the underestimation of leaf surface reflectance. As illustrated in Figure 3c,

C_{ab} estimation using P-5 for samples with high *Rs* (red points) is better than those with relatively lower *Rs* (blue points). For samples with high *Rs*, the underestimation of *Rs* using constant leaf surface reflectance in P-5 is higher than that of the sample with low *Rs*, resulting in higher offset effect on C_{ab} estimation.

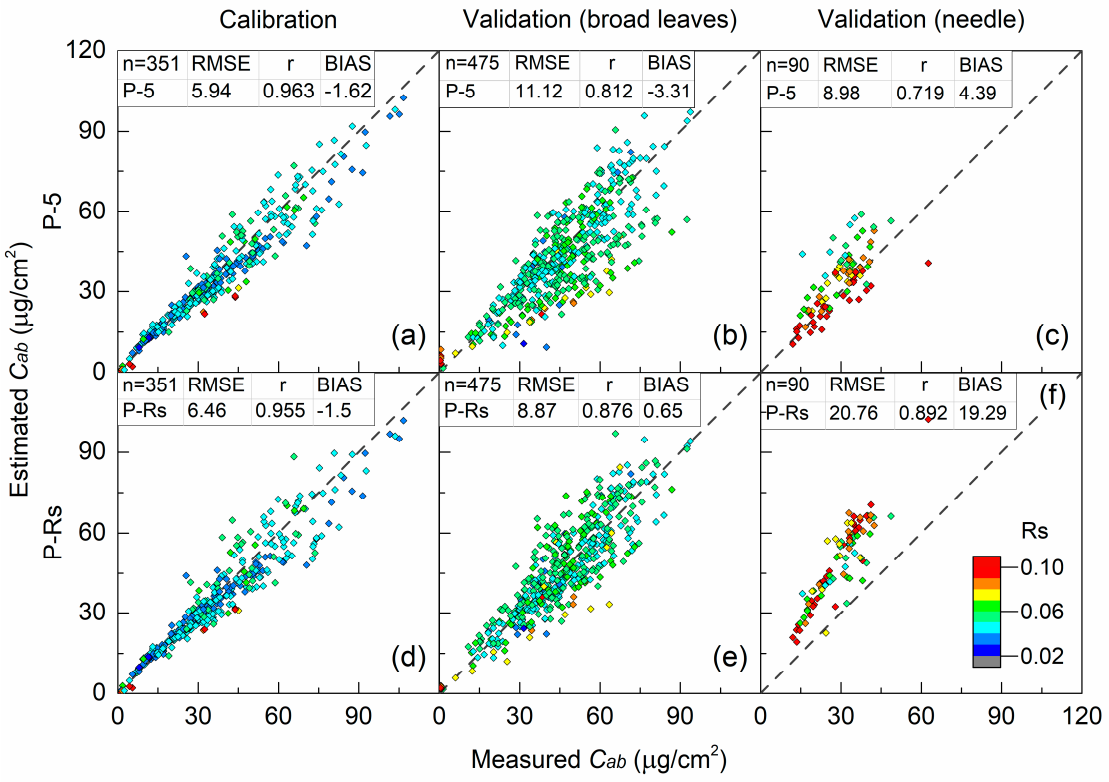

Figure 3. Estimation of chlorophyll content (C_{ab}) by inverting PROSPECT-5 (P-5) (**a**–**c**), and PROSPECT-Rsurf (P-Rs), (**d**–**f**) for calibration (the left column), broad leaves in validation datasets (the middle column) and needle leaves in validation datasets (the right column). The color of the points corresponds to the reflectance of the surface layer (*Rs*). The units of root mean square error (RMSE) and bias (BIAS) are µg/cm^2. All the correlations are significant at 0.01 level.

In order to further investigate the ability of the improved model for estimating needle chlorophyll content, we incorporated the edge effects of needles using the methods proposed in [33] in the modified model PROSPECT-Rsurf. According to [33], needle width and thickness, were introduced into the model to take into account the effects of leaf morphology on C_{ab} retrieval. The performance of C_{ab} estimation was improved by considering the edge effects in PROSPECT-Rsurf (P-Rs-edge), as demonstrated in Figure 4. The overestimation of C_{ab} is alleviated compared to PROSPECT-Rsurf in Figure 3f. The RMSE using P-Rs-edge decreases from 8.98 to 6.08 µg/cm2, with *r* increasing from 0.72 to 0.77, and BIAS adjusted from 4.39 to −1.61, compared to that of PROSPECT (P-5). C_{ab} estimated using P-Rs-edge is also better than the results of incorporating the edge effects without considering the variation of leaf surface reflectance demonstrated in [33] (RMSE = 6.32 µg/cm^2, r = 0.77), with the scattered points closer to the 1:1 line.

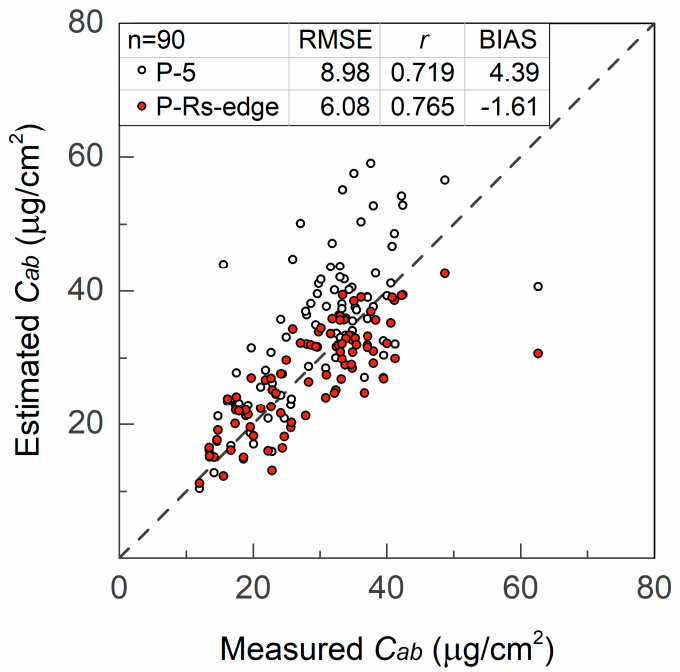

Figure 4. Estimation of needle chlorophyll content (Cab) by considering the edge effects in PROSPECT-Rsurf (P-Rs-edge, red circles) and PROSPECT-5 (P-5, black hollow circles). The units of RMSE and BIAS are µg/cm^2. All the correlations are significant at 0.01 level.

4.1.3. Spectra Reconstruction

We compared the spectral RMSE and *r* between the measured spectra and spectra reconstructed by PROSPECT-5 (P-5) and PROSPECT-Rsurf (P-Rs) after model inversion on calibration and validation datasets (Figure 5). RMSE for broadleaf validation leaves obtained with P-5 ranges from 0.01 to 0.03 over 400–800 nm, while for needle leaves RMSE (P-5) is between 0.01 and 0.05 over the VIS and is much higher (>0.06) over the NIR. P-Rs outperforms P-5 over 400-800 nm for both broad and needle samples, with RMSEs decline to lower than 0.015. P-Rs greatly improve *R* simulation over the VIS for broad leaves. For needle leaves, RMSEs for both *R* and *T* decline greatly over 400-800 nm, while the improvement over NIR for needle leaves is predominant with RMSE decreased from over 0.06 to less than 0.01. There are great increases in *r* for *R* from 400–700 nm especially over 400–500 nm, whereas the improvements of *r* for *T* is minor. The reconstructed *R* is highly correlated to measurements with *r* close to 0.9.

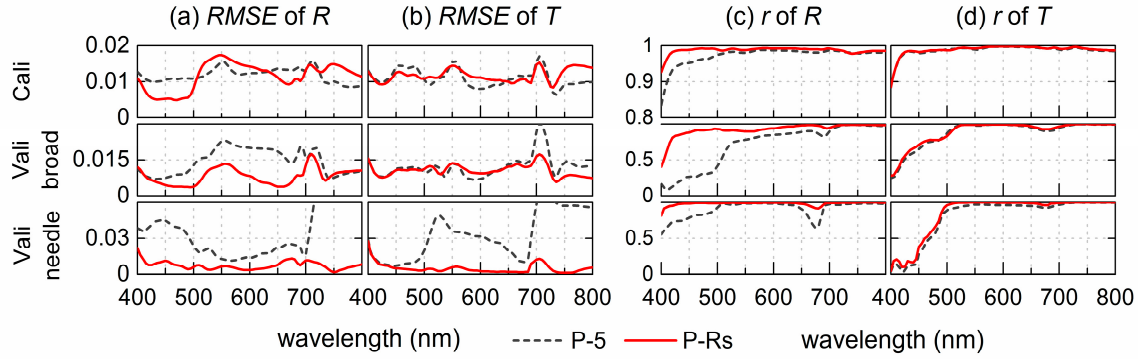

Figure 5. Spectral RMSE and Pearson's correlation coefficient (*r*) between the measured and simulated leaf reflectance (*R*) and transmittance (*T*) obtained for the calibration and validation datasets corresponding to the three groups in Figure 3 after model inversion using PROSPECT-5 (P-5) and PROSPECT-Rsurf (P-Rs).

To further illustrate the ability of PROSPECT-Rsurf to simulate leaf optical properties, we selected samples with a large range of C_{ab} and relatively high *Rs* values (Figure 6). For the samples with C_{ab} ranging from 0.9 to 80.9 μg/cm^2, *R* and *T* simulated values using P-Rs are quite close to the measured ones. In most cases, the fit using P-Rs is better than that using P-5, especially where *Rs* values are high. For example, the measured reflectance spectra of *Cornus alba 'Elegantissima'* and *Eucalyptus gunnii* leaves (Figure 6c,e) are high compared to other leaves with similar C_{ab} values, probably due to the high surface reflectance. *R* of the two leaves is substantially underestimated by P-5 over 400–700 nm and *T* is also underestimated around 550 nm. The underestimation is greatly reduced using P-Rs for both *R* and *T*.

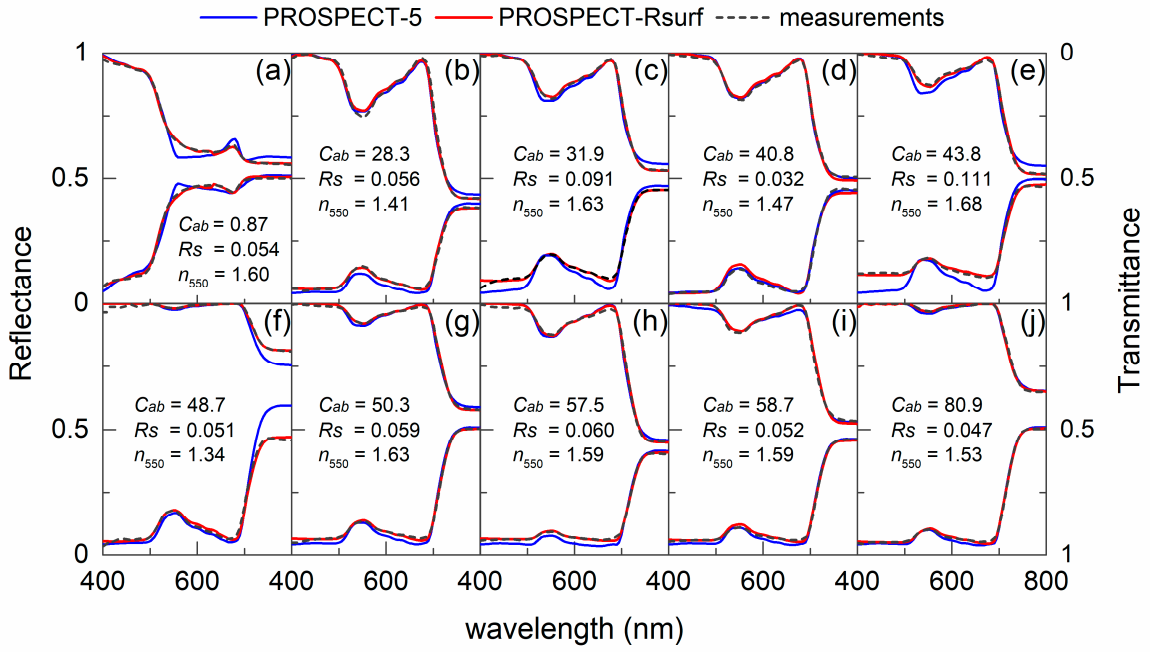

Figure 6. The measured (black dash line) versus simulated (blue line for PROSPECT-5 and red line for PROSPECT-Rsuf) reflectance (lower spectra) and transmittance (upper spectra). These samples include leaves with both low and high *N* and C_{ab} values. The measured C_{ab} and estimated *Rs* and n_{in} at 550 nm (n_{550}) values are listed in the plots. The unit of C_{ab} is μg/cm^2. Species for the plots are (**a**) *Robinia pseudoacacia 'Frisia'*, (**b**) *Zea mays*, (**c**) *Cornus alba 'Elegantissima'*, (**d**) *Triticum aestivum*, (**e**) *Eucalyptus gunnii*, (**f**) *Picea mariana* (Mill.), (**g**) *Salix atrocinerea*, (**h**) *Populus nigra*, (**i**) *Alnus glutinosa*, and (**j**) *Ligustrum lucidum*, respectively.

4.2. Estimated Leaf Surface Reflectance and Refractive Indices

Leaf surface layer reflectance estimated during the inversion process for all the leaves derived from Equation (9) is illustrated in Figure 7. The nearly flat lines of *Rs* indicate that spectral variation of the estimated *Rs* is minor, with the mean standard deviation of 0.0025 over 400–800 nm. The histogram (Figure 7b) shows that *Rs* values at 550 nm for most samples range from 0.03 to 0.07, with a mean value of 0.0527. *Rs* can account for a large proportion of leaf total reflectance in VIS. Distributions of the ratio of *Rs* to leaf total reflectance at 550 nm (R_{550}) and 680 nm (R_{680}), respectively, for all the samples are shown in Figure 7c. The average proportion of *Rs* to R_{550} is 39.8%, and for more than 90% samples the proportion of *Rs* to R_{550} is between 15% and 65%. The proportion of *Rs* to R_{680} is even higher than that of *Rs* to R_{550}, with an average proportion to be 86.3% and more than 75% samples having the *Rs*-to-R_{680} ratio higher than 80%.

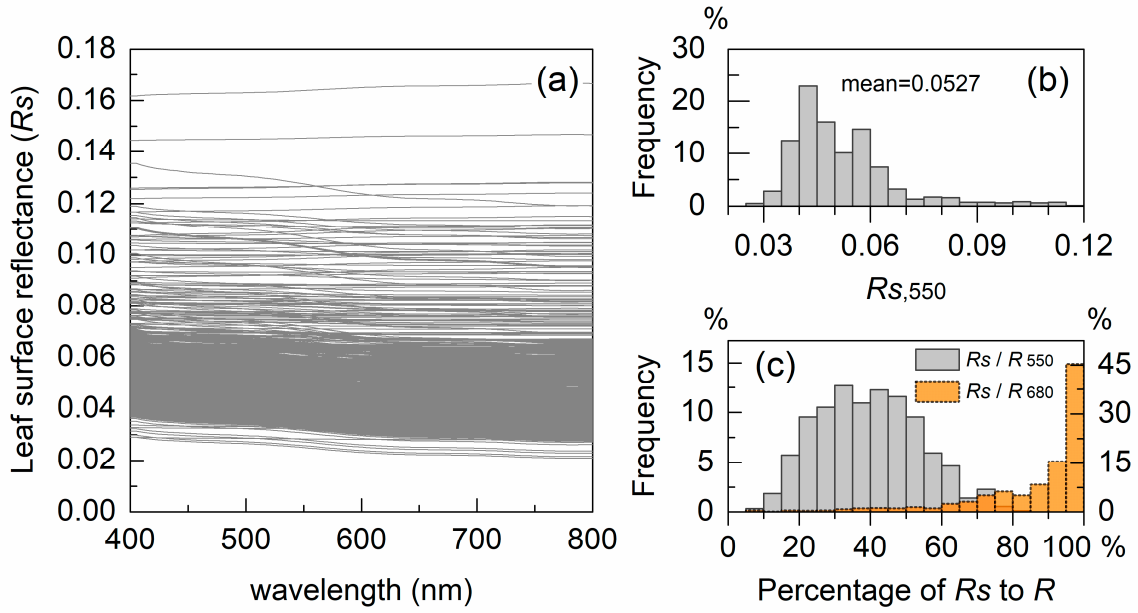

Figure 7. (**a**) Estimated leaf surface layer reflectance (*Rs*) for all leaf samples. (**b**) Distribution of *Rs* at 550 nm for all the samples. (**c**) Distribution of the proportion of *Rs* to leaf total reflectance at 550 nm (grey bars) and 680 nm (orange bars), respectively.

Statistics of the mean values of estimated *Rs* at 550 nm ($Rs_{,550}$) for each species are shown in Figure 8 and Table A2. About 93% of all 56 species under study have mean $Rs_{,550}$ in the range from 0.03 to 0.05. The mean reflectance of the upper boundary layer in PROSPECT-5 from 400–800 nm (r_a = 0.037) is also in this range. Among these species, mean $Rs_{,550}$ of leaves of cider gum (*Eucalyptus gunnii*), black spruce (*Picea mariana* (Mill.)), and red-barked dogwood (*Cornus alba 'Elegantissima'*) are much higher than others, at 0.112, 0.082, and 0.080, respectively. The high *Rs* can be ascribed to the presence of epicuticular wax that reflects a large amount of incident light [11,22,24]. Further investigation into the surface characteristics of leaves with high *Rs* reveals that leaves with heavy wax on the surface, or leathery or hard leaves with glabrous surfaces (Table A2 and Figure A1 in the Appendix A) usually have high *Rs*. Leaves of leatherleaf arrowwood (*Viburnum rhytidophyllum*) are lustrous but the estimated surface reflectance is not very high (mean $Rs_{,550}$ = 0.042), probably due to the deeply veined surface which increases the surface roughness and reduces surface specular reflectance. The estimated *Rs* of some pubescence leaves is also high, although not as high as waxy leaves. These results demonstrate that the estimated *Rs* is able to represent the main reflectance characteristics of leaf surfaces.

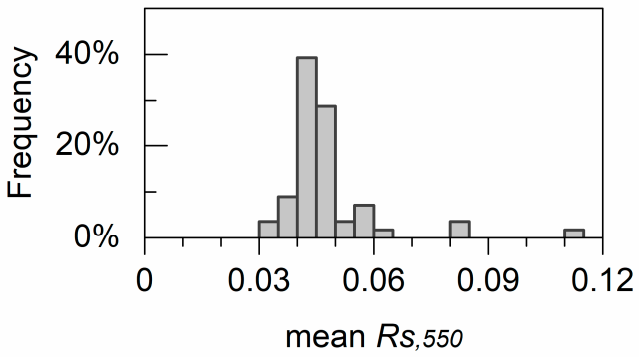

Figure 8. Histogram of mean 550 nm leaf surface layer reflectance (*Rs*) values of the 56 plant species.

The estimated *Rs* is found to be strongly correlated to leaf reflectance around 445 nm (R_{445}), except for broad leaves with extremely low Cab (<2 μg/cm^2, black cross in Figure 9). There is a slight difference in the R_{445} and *Rs* relationship between broad and needle leaves.

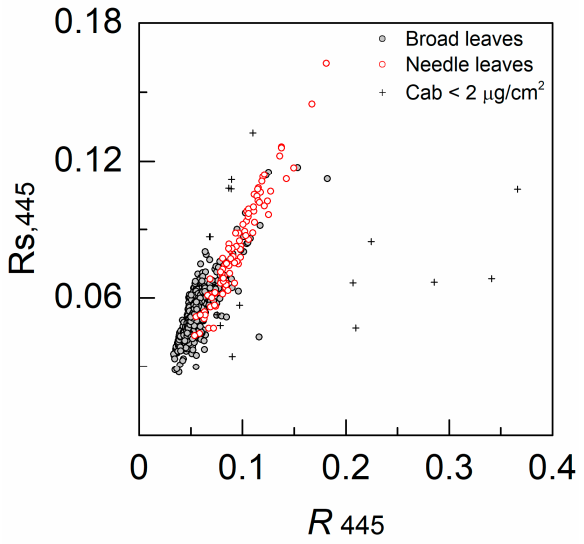

Figure 9. Relationship between *Rs* ($Rs_{,445}$) and leaf reflectance at 445 nm (R_{445})). The black crosses refer to the broad leaves with Cab lower than 2 μg/cm^2.

The estimated leaf interior refractive index (n_{in}) is demonstrated in Figure 10. For most of the samples, n_{in} values are in the range from 1.2 to 2.0. The refractive index used in PROSPECT-3 and PROSPECT-5 are in the range of the estimated leaf interior refractive indices. Similar to the refractive index used in PROSPECT-3 and PROSPECT-D, spectral variation of the estimated leaf interior refractive index is minor. The estimated spectra of n_{in} conform with the leaf refractive indices derived from K–K relations [39].

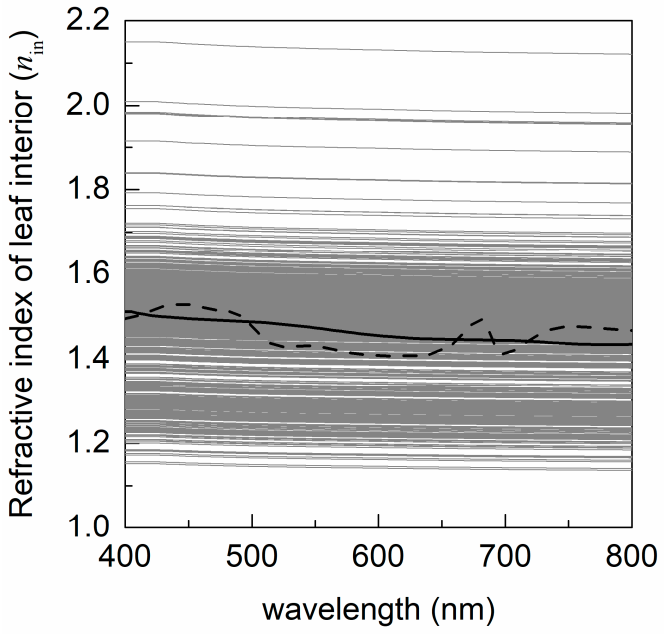

Figure 10. The estimated leaf interior refractive index (n_{in}) for all the samples over 400 to 800 nm. The curves of the leaf refractive index used in PROSPECT-3 (black solid line) and PROSPECT-5 (black dash line) are demonstrated for comparison.

4.3. Sensitivity to the Uncertainty Associated with Rs

4.3.1. Global Sensitivity Analysis

The results of Sobol's sensitivity analysis for the total reflectance (R) and transmittance (T) simulated using PROSPECT-Rsurf are shown in Figure 11. Leaf chlorophyll content (C_{ab}) mainly influences R and T in the range over 500 to 750 nm, while N mainly affects the NIR spectrum (750–800 nm). The effects of leaf carotenoids content (C_{ar}) on R and T are minor, mainly over 450 to 550 nm, while leaf dry matter content (LMA) mainly contributes to the absorption in NIR. The internal refractive index (represented by f_{in}) can be considered as another variable influencing the leaf internal structure and contributes to R and T mainly over NIR. Leaf surface reflectance (Rs), represented by the ratio of the refractive index of leaf surface layer to that of interior layers (f'_{surf}), is the main factor contributing to R at blue wavelengths (400–500 nm), and has little contribution to T. In the red-edge region over 690–720 nm, C_{ab} and N are the two main contributors, while the influence of Rs (i.e., f'_{surf}) on R is low. The red edge reflectance is more sensitive to variations in C_{ab} and N rather than in Rs.

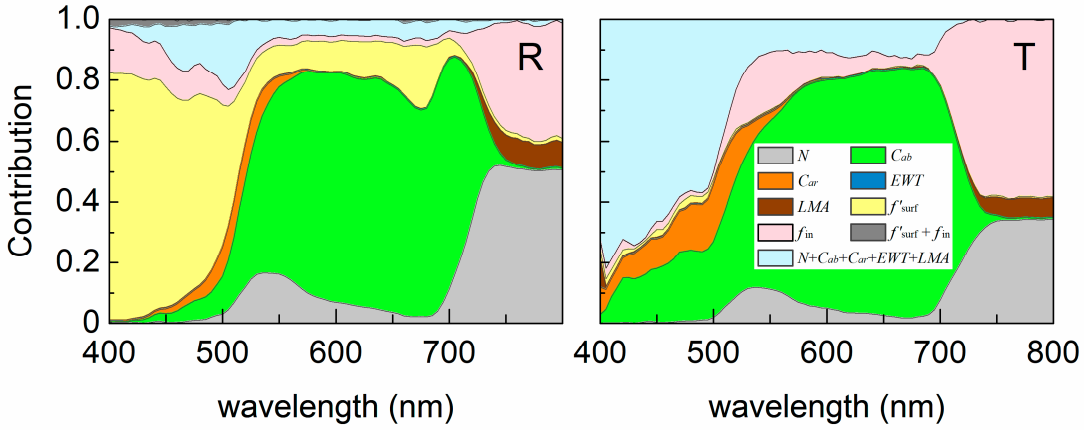

Figure 11. First order sensitivity coefficients of the input variables and their interactions to total leaf reflectance (R, left) and transmittance (T, right) for PROSPECT-Rsurf. N is the leaf structure parameter, Cab, Car, LMA, and EWT are the biochemical contents, and f'_{surf} and f_{in} are the two factors related to the refractive index of leaf surface and interior materials, respectively.

4.3.2. Sensitivity of Model Calibration

After adding groups of noise to the measured spectra, group values of N, n_{surf}, and n_{in} and the corresponding Rs are obtained for each sample. The distributions of the coefficient of variability (CV) of N, n_{surf}, n_{in}, and Rs are shown in Figure 12. Most CV values of N are lower than 2.5%, with a mean value of 1.0%. The max CV of n_{surf} and n_{in} are lower than 1.5%, and the mean values are less than 0.5%. The CV values of the corresponding Rs calculated from n_{surf} and n_{in} are between 0.4% to 1.4%.

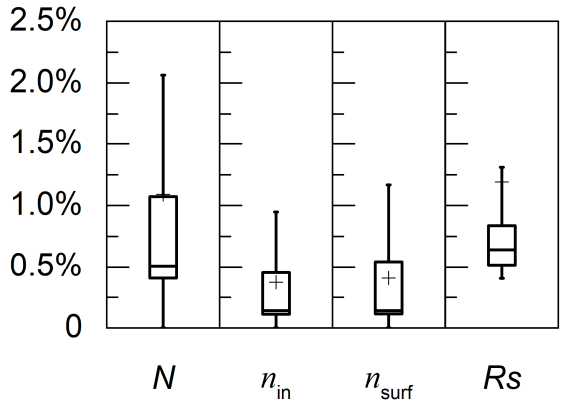

Figure 12. Distributions of the coefficient of variability (CV) of retrieved N, n_{surf}, n_{in}, and Rs after adding noise to measured R and T and repeating the inversion 100 times. Cross marks correspond to the mean values.

The variability in SACs of chlorophyll (k_{Cab}) derived from noisy f'_{surf} and f_{in} (corresponding to n_{surf} and n_{in}, respectively) is limited to the 400–450 nm wavelength range, while that of carotenoids (k_{Cxc}) is in 400–480 nm (Figure 13). The influence of introducing noises to noisy f'_{surf} and f_{in} on k_{Cab} is lower than that on k_{Cxc}. The mean standard deviation (σ) of k_{Cab} and k_{Cxc} over 400–450 nm is 0.0016 (CV = 4.6%) and 0.0052 (CV = 14.2%), respectively.

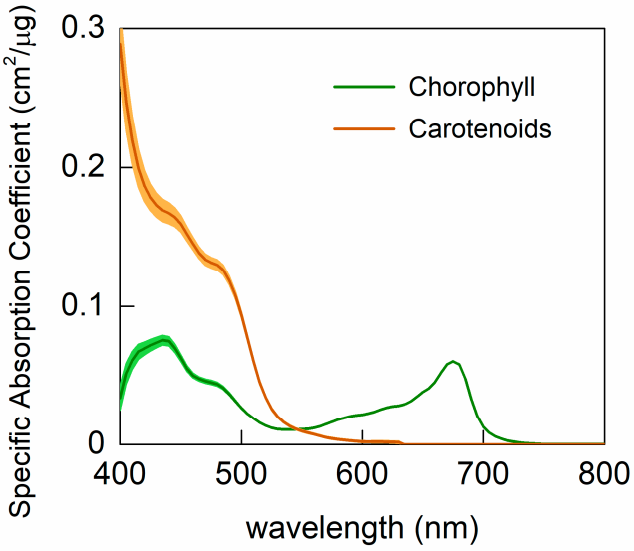

Figure 13. Comparison of the SACs obtained for total chlorophyll (green) and carotenoids (orange) when adding noise to retrieved Rs values (100 repetitions; plain lines and their envelope correspond to mean value ±1 standard deviation).

4.3.3. Chlorophyll Content Retrieval

C_{ab} retrieved using PROSPECT-Rsurf with the noisy f'_{surf} and f_{in} (corresponding to n_{surf} and n_{in}, respectively) are illustrated in Figure 14. For the calibration dataset, the performance of PROSPECT-Rsurf (P-Rs) and PROSPECT-5 (P-5) are comparable, and it introduces slight uncertainty in C_{ab} estimation after adding noise to f'_{surf} and f_{in}. For broadleaf validation samples (V(b) in Figure 14), the uncertainty in C_{ab} estimation using P-Rs with noise added is small. RMSE changes from 8.90 to 10.81 µg/cm^2 with a mean value of 9.63 (8.6% increase comparing to that of P-Rs), and r varies from 0.85–0.88 (mean = 8.71). Nevertheless, C_{ab} retrieval using P-Rs with noises introduced is still better than that of P-5 (RMSE = 11.12 µg/cm^2, r = 0.81), with lower RMSE and higher r values. It proves that P-Rs is effective and better than P-5 in C_{ab} estimation for tested broadleaf samples. For black

spruce needles (V(n)) with relatively high surface reflectance, wide variations in RMSE are found, indicating that C_{ab} estimation for needles is sensitive to the noise added to f'_{surf} and f_{in}. However, the estimated C_{ab} using P-Rs is better correlated with measurements than that using P-5, no matter noise is introduced or not. As mentioned before there is an overestimation of leaf spectra since the edge effects are ignored, leading to systematic overestimation of retrieved C_{ab}. This systematic error in C_{ab} can explain the higher RMSE by P-Rs than by P-5.

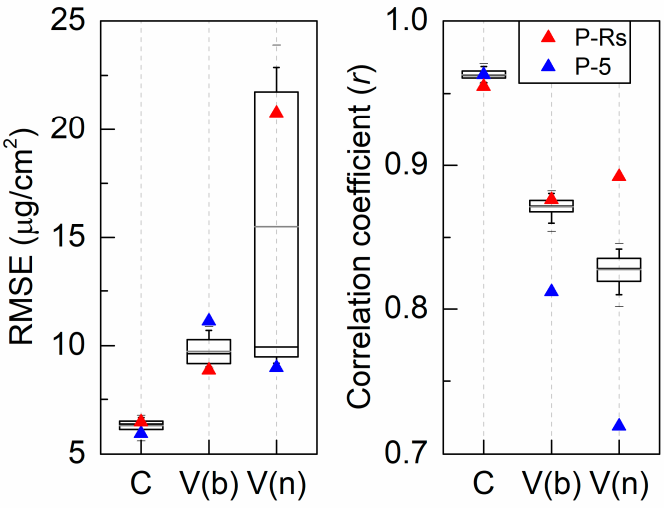

Figure 14. Distribution of the RMSE and Pearson's correlation coefficient (r) between the measured and estimated chlorophyll content after adding noise to f'_{surf} and f_{in} for calibration (C), broadleaf validation (V(b)), and needle validation (V(n)) datasets using PROSPECT-Rsurf (P-Rs). Colored markers correspond to the RMSE or r obtained from PROSPECT-Rsurf (P-Rs) and PROSPECT-5 (P-5) when no noise is added.

5. Discussion

5.1. Effects of Leaf Surface Reflectance on Chlorophyll Estimation

The existing versions of PROSPECT were proved to be effective for retrieving foliar biochemical contents for the majority of the tested samples. However, the spectral fit and pigments retrieval using PROSPECT models are poor for leaves with extremely high surface reflectance [22,24]. In this study, we incorporate variable leaf surface reflectance in PROSPECT-Rsurf to improve chlorophyll content (C_{ab}) retrieval and spectral reconstruction, especially for samples coated with heavy wax or hard cuticle leading to high leaf surface reflectance. Leaf surface reflectance can occupy over 40% of the total reflectance at around 550 nm, and large variations across different species and plant functional types are observed, indicating the important influence of leaf surface reflectance on leaf chlorophyll content retrieval.

PROSPECT-5 and PROSPECT-Rsurf performed similarly in C_{ab} retrieval for leaves with lower *Rs*, since the slight differences between the leaf surface reflectance used in the two models were compensated by adjusting the structure parameter N during model inversion. However, when the actual leaf surface reflectance is much higher than the surface reflectance used in PROSPECT-5, the error in spectral simulation probably cannot be compensated by adjusting N during inversion, leading to error in C_{ab} estimation. Notwithstanding the compensating effects of N adjustment on C_{ab} estimation using PROSPECT-5, PROSPECT-Rsurf shows notable improvements in C_{ab} estimation as well as spectral simulation over 400–800 nm. Two new variables representing leaf surface and interior refractive indices are introduced in PROSPECT-Rsurf. The inversion procedure may consequently increase the computing time and the applicability of the model at the canopy scale is limited as the additional parameters may increase the ill-posed problem of model inversion. However, we demonstrate that the

leaf surface reflectance effect on chlorophyll content retrieval can be alleviated by introducing variable leaf surface layer reflectance.

Sensitivity analysis shows that leaf reflectance at the red-edge region (690–720 nm) is found to be less sensitive to the variation of *Rs* than that at other VIS wavelengths (Figure 11), suggesting that the red-edge reflectance can be used to build spectral indices that is less sensitive to leaf surface reflectance variation. This agrees with the spectral indices for C_{ab} estimation developed from empirical data in previous studies [4,16]. The difference between the reflectance at two VIS bands reduced the effect of surface reflectance, since surface reflectance was considered as wavelength independent. Sims and Gamon [5] found that modified spectral indices incorporating reflectance at 445 nm (R_{445}) is able to eliminate the effect of surface reflectance and is better correlated with chlorophyll content. The high correlation between leaf surface layer reflectance and R_{445} found in this study provides support for these spectral indices from the perspective of a radiative transfer model.

The improvement in chlorophyll estimation and spectral reconstruction using PROSPECT-Rsurf is important for the study of the interaction between photosynthetic pigments and solar radiation. Given that leaf chlorophyll content can drive about 60% of the canopy reflectance variation in VIS [43], the effects of variable leaf surface reflectance on canopy reflectance in VIS cannot be ignored. Future studies by coupling PROSPECT-Rsurf with canopy models are needed to explore the influence of leaf surface reflectance on canopy reflectance and therefore canopy chlorophyll content retrieval.

5.2. Improvements on Needle Leaf Chlorophyll Content Retrieval

When applying PROSPECT-5 to needle leaves, the amount of light that escapes from needle edges cannot be ignored. In PROSPECT-5 inversion the overestimation of leaf *R* and *T* caused by the edge effects is partially compensated by the underestimation of leaf surface reflectance. Therefore, C_{ab} estimation using PROSPECT-5 appears good with low BIAS. When leaf surface reflectance is adjusted in PROSPECT-Rsurf, the edge effects show up, leading to the overestimation in C_{ab} but higher correlation coefficients compared to measurements. Zhang et al. [33] introduced needle width and thickness in a scheme to adjust measured leaf total reflectance and transmittance for considering the edge effects on chlorophyll content retrieval, and showed that C_{ab} estimation is improved compared to that of PROSPECT-3. Based on this study, we incorporated the edge effects of needles in PROSPECT-Rsurf. The performance of C_{ab} is improved after considering both leaf edge and surface effects, compared to both PROSPECT-5 and the results in [33]. The result indicates that appropriate representation of needle structure is required in order to estimate needle chlorophyll content with good accuracy. There are still large uncertainties in the estimated C_{ab} compared to measurements. This necessitates further model refinements specific for the morphology and internal structure of needle samples, as well as accurate measurements of needle spectra.

5.3. Leaf Surface Reflectance and Refractive Indices

The estimated *Rs* differs widely for leaves with different surface features. Our results show that some leaves with heavy wax or hard cuticle, or white trichomes, usually have high leaf surface reflectance. Leaf surfaces coated with heavy waxes or hard cuticle reflect large amounts of light, most of which is specular, while trichomes increase the ability to scatter light [11]. However, due to the variety of the morphology and density of epicuticular waxes or trichomes, quantitative evaluation of the effects of waxes and trichomes on leaf total reflectance is difficult and needs further exploration.

The surface layer reflectance (*Rs*) is characterized by the refractive indices of the additional surface layer (n_{surf}) and the interior layers (n_{in}) in PROSPECT-Rsurf. The leaf surface layer and interior refractive indices derived from model inversion are comparable to the leaf refractive index obtained by Kramers–Kronig (K–K) transformations [39]. The derived leaf surface and interior layer refractive indices should not be considered as true representations of leaf surface and interior refractive indices but as equivalent parameters compensating for leaf surface reflectance and internal multiple scattering, respectively. The spectral variations of n_{surf} and n_{in} are minor, resulting in relatively flat leaf surface

layer reflectance spectra in 400–800 nm, which are consistent with the findings that leaf specular reflectance from a surface is usually considered as wavelength-independent [13], as the cuticle and cell walls of leaf epidermis usually contain no pigments [7].

The improvements in spectral reconstruction and chlorophyll content retrieval using PROSPECT-Rsurf suggest that the leaf surface reflectance obtained in this study is a better estimate of the actual surface reflectance than the original reflectance spectrum used in PROSPECT-5. The derived surface layer reflectance is effective in revealing the variations in leaf surface reflectance features across different species, functional types and growing stages. Therefore, although a certain degree of uncertainty exists in the estimated *Rs*, we believe that the surface layer reflectance estimated in this study is reasonably accurate. Measurements on the surface reflectance and quantitative evaluation of the two refractive indices are needed to further validate our modified model and develop methods to nondestructively estimate the surface reflectance more accurately for pigments retrieval.

6. Conclusions

In this study, we demonstrated that incorporating variable leaf surface layer reflectance in the PROSPECT-Rurf model is effective in improving the leaf chlorophyll content retrieval as well as spectral simulation, especially for leaves with high surface reflectance. The root mean square error (RMSE) of C_{ab} estimates decreased from 11.1 μg/cm^2 to 8.9 μg/cm^2 and the Pearson's correlation coefficient (r) increased from 0.81 to 0.88 ($p < 0.01$) for broadleaf samples in validation datasets, compared to PROSPECT-5. For needle leaves, r increased from 0.71 to 0.89 ($p < 0.01$), but systematic overestimation of C_{ab} was found to be due to the edge effects of needles. After incorporating the edge effects in PROSPECT-Rsurf, the overestimation of C_{ab} was alleviated and its estimation was improved. The result indicates that accurate representation of needle structure is required in order to appropriately estimate C_{ab}.

Although a certain degree of uncertainty exists, the estimated *Rs* is able to capture the variation of leaf surface reflection features across different plant species. Sensitivity analysis indicated that the influence of the uncertainty in estimation of *Rs* on chlorophyll content retrieval is small (8.6% increase on average). The estimated leaf surface reflectance was found to be highly correlated with leaf total reflectance at 445 nm (R_{445}), providing evidence for using R_{445} in spectral indices to eliminate the effect of surface reflectance on C_{ab} estimation. We also found that the red-edge leaf reflectance is less sensitive to variation in leaf surface reflectance, confirming the usefulness of red-edge wavelengths for chlorophyll retrieval.

The coupling of PROSPECT-Rsurf with canopy models will allow exploration of the influence of leaf surface reflectance on canopy reflectance and therefore canopy chlorophyll content retrieval, for the purpose of monitoring plant physiological statuses and vegetation productivity across different spatial and temporal scales.

Author Contributions: Conceptualization, F.Q.; formal analysis, F.Q.; funding acquisition, W.J.; investigation, F.Q., H.C., J.L., Q.Z. and Y.Z.; methodology, F.Q.; supervision, J.C.; writing—original draft, F.Q.; writing—review and editing, J.C., H.C., Q.Z., Y.Z. and W.J.

Funding: This research was funded by the National Key R&D Program of China, grant number 2016YFA0600202; National Natural Science Foundation of China, grant number 41701393; Natural Science Foundation of Jiangsu Province for Youth, grant number BK20170641; and China Postdoctoral Science Foundation, grant number 2018T110477 and 2017M621698.

Acknowledgments: We thank Luc Bidel, Christophe François and Gabriel Pavan who collected and shared the ANGERS dataset. We are indebted to Jun Wang, Meihong Fang, and some other group members at Nanjing University who are not listed here, for their great help in the leaf biochemical and spectral measurements.

Conflicts of Interest: The authors declare no conflict of interest. The funders had no role in the design of the study; in the collection, analyses, or interpretation of data; in the writing of the manuscript, or in the decision to publish the results.

Appendix A

Table A1. List of symbols used in this study.

N	The structure parameter in PROSPECT
C_{ab}	Leaf total chlorophyll content
C_{xc}	Leaf total carotenoids content
EWT	Equivalent water thickness (leaf water content)
LMA	Leaf mass per area (leaf dry matter content)
R	Leaf total directional-hemispherical reflectance
T	Leaf total directional-hemispherical transmittance
Rs	Leaf surface layer reflectance
$n_{P3}\,(\lambda)$	The refractive index used in PROSPECT-3
$n_{surf}\,(\lambda)$	The refractive index of the surface layer
$n_{in}\,(\lambda)$	The refractive index of interior layers
f'_{surf}	$n_{surf}\,(\lambda) / n_{in}\,(\lambda)$
f_{in}	$n_{in}\,(\lambda) / n_{P3}\,(\lambda)$

Table A2. Estimated *Rs* at 550 nm and leaf surface characteristics of species with high *Rs*.

ID	Species (Latin Name)	*Rs*			Characteristics of Leaf Upper Surface
		Mean	Min	Max	
(a)	*Eucalyptus gunnii*	0.112	0.111	0.112	waxy; grey-green; thick
(b)	*Picea mariana* (Mill.)	0.082	0.042	0.164	waxy; needle
(c)	*Cornus alba 'Elegantissima'*	0.080	0.069	0.095	glabrous green; pubescent with short white appressed trichomes
(d)	*Triticum aestivum*	0.063	0.036	0.093	waxy, or pubescent
(e)	*Zea mays*	0.057	0.050	0.065	waxy, or pubescent
(f)	*Schefflera arboricola 'Gold Capella'*	0.057	0.028	0.075	leathery; glabrous
(g)	*Populus nigra*	0.055	0.047	0.060	thin leathery; glabrous
(h)	*Alnus glutinosa*	0.054	0.049	0.059	leathery; glabrous; dark green
(i)	*Populus alba*	0.052	0.050	0.054	glabrous
(j)	*Ilex aquifolium 'Golden Milkboy'*	0.049	0.049	0.049	leathery; shiny; dark green; hard
(k)	*Salix atrocinerea*	0.048	0.047	0.051	dull or slightly glossy; pubescent or pilose (hairs white)
(l)	*Cyclocarya paliurus*	0.046	0.044	0.049	glabrous
(m)	*Quercus acutissima*	0.045	0.037	0.057	glabrous
(n)	*Ligustrum lucidum*	0.044	0.039	0.050	leathery or papery; glabrous
(o)	*Liquidambar formosana*	0.044	0.040	0.054	glabrous

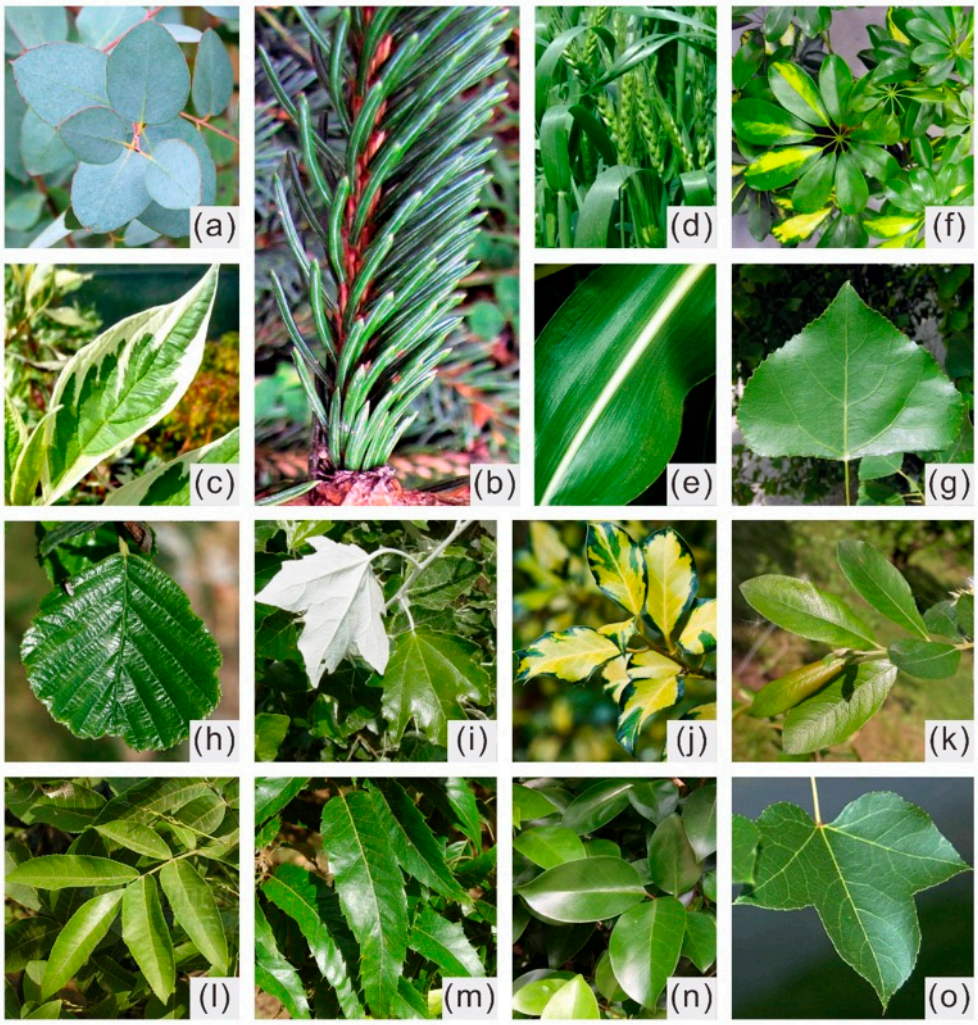

Figure A1. Pictures of leaves of species with high estimated surface reflectance (Rs-vi). The species of leaves in each picture numbered with letters from (**a**) to (**o**) correspond to the species ID in the first column of Table A2.

References

1. Comar, A.; Baret, F.; Obein, G.; Simonot, L.; Meneveaux, D.; Viénot, F.; de Solan, B. ACT: A leaf BRDF model taking into account the azimuthal anisotropy of monocotyledonous leaf surface. *Remote Sens. Environ.* **2014**, *143*, 112–121. [CrossRef]
2. Bousquet, L.; Lachérade, S.; Jacquemoud, S.; Moya, I. Leaf BRDF measurements and model for specular and diffuse components differentiation. *Remote Sens. Environ.* **2005**, *98*, 201–211. [CrossRef]
3. Maccioni, A.; Agati, G.; Mazzinghi, P. New vegetation indices for remote measurement of chlorophylls based on leaf directional reflectance spectra. *J. Photochem. Photobiol. B Biol.* **2001**, *61*, 52–61. [CrossRef]
4. Levizou, E.; Drilias, P.; Psaras, G.K.; Manetas, Y. Nondestructive assessment of leaf chemistry and physiology through spectral reflectance measurements may be misleading when changes in trichome density co-occur. *New Phytol.* **2005**, *165*, 463–472. [CrossRef] [PubMed]
5. Sims, D.A.; Gamon, J.A. Relationships between leaf pigment content and spectral reflectance across a wide range of species, leaf structures and developmental stages. *Remote Sens. Environ.* **2002**, *81*, 337–354. [CrossRef]
6. Cameron, K.D.; Teece, M.A.; Smart, L.B. Increased accumulation of cuticular wax and expression of lipid transfer protein in response to periodic drying events in leaves of tree tobacco. *Plant Physiol.* **2006**, *140*, 176–183. [CrossRef]

7. Grant, L.; Daughtry, C.S.T.; Vanderbilt, V.C. Polarized and specular reflectance variation with leaf surface features. *Physiol. Plant.* **1993**, *88*, 1–9. [CrossRef]
8. Pfündel, E.E.; Agati, G.; Cerovic, Z.G. Optical Properties of Plant Surfaces. In *Annual Plant Reviews Volume 23: Biology of the Plant Cuticle*; Blackwell Publishing Ltd.: Oxford, UK, 2006; pp. 216–249.
9. Baldini, E.; Facini, O.; Nerozzi, F.; Rossi, F.; Rotondi, A. Leaf characteristics and optical properties of different woody species. *Trees* **1997**, *12*, 73–81. [CrossRef]
10. Ehleringer, J.; Björkman, O.; Mooney, H.A. Leaf pubescence: Effects on absorptance and photosynthesis in a desert shrub. *Science* **1976**, *192*, 376–377. [CrossRef]
11. Holmes, M.G.; Keiller, D.R. Effects of pubescence and waxes on the reflectance of leaves in the ultraviolet and photosynthetic wavebands: A comparison of a range of species. *Plant Cell Environ.* **2002**, *25*, 85–93. [CrossRef]
12. Breece, H.T.; Holmes, R.A. Bidirectional Scattering Characteristics of Healthy Green Soybean and Corn Leaves in Vivo. *Appl. Opt.* **1971**, *10*, 119–127. [CrossRef] [PubMed]
13. Jay, S.; Bendoula, R.; Hadoux, X.; Féret, J.-B.; Gorretta, N. A physically-based model for retrieving foliar biochemistry and leaf orientation using close-range imaging spectroscopy. *Remote Sens. Environ.* **2016**, *177*, 220–236. [CrossRef]
14. Vanderbilt, V.C.; Grant, L. Polarization photometer to measure bidirectional reflectance factor R (55°, 0°; 55°, 180°) of leaves. *Opt. Eng.* **1986**, *25*, 1002–1012. [CrossRef]
15. Verrelst, J.; Camps-Valls, G.; Muñoz-Marí, J.; Rivera, J.P.; Veroustraete, F.; Clevers, J.G.; Moreno, J. Optical remote sensing and the retrieval of terrestrial vegetation bio-geophysical properties—A review. *ISPRS J. Photogramm. Remote Sens.* **2015**, *108*, 273–290. [CrossRef]
16. Gitelson, A.A.; Gritz, Y.; Merzlyak, M.N. Relationships between leaf chlorophyll content and spectral reflectance and algorithms for non-destructive chlorophyll assessment in higher plant leaves. *J. Plant Physiol.* **2003**, *160*, 271–282. [CrossRef]
17. Croft, H.; Chen, J.M.; Zhang, Y. The applicability of empirical vegetation indices for determining leaf chlorophyll content over different leaf and canopy structures. *Ecol. Complex.* **2014**, *17*, 119–130. [CrossRef]
18. Jacquemoud, S.; Baret, F. PROSPECT: A model of leaf optical properties spectra. *Remote Sens. Environ.* **1990**, *34*, 75–91. [CrossRef]
19. Combal, B.; Baret, F.; Weiss, M.; Trubuil, A.; Macé, D.; Pragnère, A.; Myneni, R.; Knyazikhin, Y.; Wang, L. Retrieval of canopy biophysical variables from bidirectional reflectance: Using prior information to solve the ill-posed inverse problem. *Remote Sens. Environ.* **2003**, *84*, 1–15. [CrossRef]
20. Darvishzadeh, R.; Skidmore, A.; Schlerf, M.; Atzberger, C. Inversion of a radiative transfer model for estimating vegetation LAI and chlorophyll in a heterogeneous grassland. *Remote Sens. Environ.* **2008**, *112*, 2592–2604. [CrossRef]
21. Jacquemoud, S.; Ustin, S.L.; Verdebout, J.; Schmuck, G.; Andreoli, G.; Hosgood, B. Estimating Leaf Biochemistry Using the PROSPECT Leaf Optical Properties Model. *Remote Sens. Environ.* **1996**, *56*, 194–202. [CrossRef]
22. Barry, K.; Newnham, G. Quantification of chlorophyll and carotenoid pigments in eucalyptus foliage with the radiative transfer model PROSPECT 5 is affected by anthocyanin and epicuticular waxes. In Proceedings of the Geospatial Science Research Symposium—GSR_2, Melbourne, Australia, 10–12 December 2012; pp. 1–7.
23. Barry, K.M.; Newnham, G.J.; Stone, C. Estimation of chlorophyll content in Eucalyptus globulus foliage with the leaf reflectance model PROSPECT. *Agric. For. Meteorol.* **2009**, *149*, 1209–1213. [CrossRef]
24. Féret, J.B.; Gitelson, A.A.; Noble, S.D.; Jacquemoud, S. PROSPECT-D: Towards modeling leaf optical properties through a complete lifecycle. *Remote Sens. Environ.* **2017**, *193*, 204–215. [CrossRef]
25. Li, D.; Cheng, T.; Jia, M.; Zhou, K.; Lu, N.; Yao, X.; Tian, Y.; Zhu, Y.; Cao, W. PROCWT: Coupling PROSPECT with continuous wavelet transform to improve the retrieval of foliar chemistry from leaf bidirectional reflectance spectra. *Remote Sens. Environ.* **2018**, *206*, 1–14. [CrossRef]
26. Gerber, F.; Marion, R.; Olioso, A.; Jacquemoud, S.; Ribeiro da Luz, B.; Fabre, S. Modeling directional–hemispherical reflectance and transmittance of fresh and dry leaves from 0.4 µm to 5.7 µm with the PROSPECT-VISIR model. *Remote Sens. Environ.* **2011**, *115*, 404–414. [CrossRef]
27. Clark, J.B.; Lister, G.R. Photosynthetic Action Spectra of Trees. *Plant Physiol.* **1975**, *55*, 407–413. [CrossRef] [PubMed]

28. Féret, J.-B.; François, C.; Asner, G.P.; Gitelson, A.A.; Martin, R.E.; Bidel, L.P.R.; Ustin, S.L.; le Maire, G.; Jacquemoud, S. PROSPECT-4 and 5: Advances in the leaf optical properties model separating photosynthetic pigments. *Remote Sens. Environ.* **2008**, *112*, 3030–3043. [CrossRef]
29. Lichtenthaler, H.K. Chlorophylls and carotenoids: Pigments of photosynthetic biomembranes. *Methods Enzymol.* **1987**, *148*, 350–381.
30. Minocha, R.; Martinez, G.; Lyons, B.; Long, S. Development of a standardized methodology for quantifying total chlorophyll and carotenoids from foliage of hardwood and conifer tree species. *Can. J. For. Res.* **2009**, *39*, 849–861. [CrossRef]
31. Zarco-Tejada, P.J.; Miller, J.R.; Harron, J.; Hu, B.; Noland, T.L.; Goel, N.; Mohammed, G.H.; Sampson, P. Needle chlorophyll content estimation through model inversion using hyperspectral data from boreal conifer forest canopies. *Remote Sens. Environ.* **2004**, *89*, 189–199. [CrossRef]
32. Harron, J. Optical Properties of Phytoelements in Conifers. Master's Thesis, York University, North York, ON, Canada, 2000.
33. Zhang, Y.; Chen, J.M.; Miller, J.R.; Noland, T.L. Retrieving chlorophyll content in conifer needles from hyperspectral measurements. *Can. J. Remote Sens.* **2008**, *34*, 296–310.
34. Zarco-Tejada, P.J.; Miller, J.R.; Mohammed, G.H.; Noland, T.L. Chlorophyll Fluorescence Effects on Vegetation Apparent Reflectance: I. Leaf-Level Measurements and Model Simulation. *Remote Sens. Environ.* **2000**, *74*, 582–595. [CrossRef]
35. Croft, H.; Chen, J.M. Leaf pigment content. In *Comprehensive Remote Sensing*; Liang, S., Ed.; Elsevier: Oxford, UK, 2018; pp. 117–142.
36. Wellburn, A.R. The Spectral Determination of Chlorophylls a and b, as well as Total Carotenoids, Using Various Solvents with Spectrophotometers of Different Resolutions. *J. Plant Physiol.* **1994**, *144*, 307–313. [CrossRef]
37. Allen, W.A.; Gausman, H.W.; Richardson, A.J.; Thomas, J.R. Interaction of isotropic light with a compact plant leaf. *J. Opt. Soc. Am.* **1969**, *59*, 1376–1379. [CrossRef]
38. Lucarini, V.; Saarinen, J.; Peiponen, K.; Vartiainen, E. *Kramers-Kronig Relations in Optical Materials Research*; Rhodes, W.T., Ed.; Springer: Berlin, Germany, 2005; Volume 110, p. 162.
39. Chen, M.; Weng, F. Kramers-Kronig analysis of leaf refractive index with the PROSPECT leaf optical property model. *J. Geophys. Res.* **2012**, *117*. [CrossRef]
40. D'Errico, J. Fminsearchbnd. MATLAB Central File Exchange. 2012. Available online: https://ww2.mathworks.cn/matlabcentral/fileexchange/8277-fminsearchbnd-fminsearchcon (accessed on 19 March 2014).
41. Gausman, H.W.; Allen, W.A.; Escobar, D.E. Refractive Index of Plant Cell Walls. *Appl. Opt.* **1974**, *13*, 109–111. [CrossRef] [PubMed]
42. Cannavó, F. Sensitivity analysis for volcanic source modeling quality assessment and model selection. *Comput. Geosci.* **2012**, *44*, 52–59. [CrossRef]
43. Jacquemoud, S.; Verhoef, W.; Baret, F.; Bacour, C.; Zarco-Tejada, P.J.; Asner, G.P.; François, C.; Ustin, S.L. PROSPECT + SAIL models: A review of use for vegetation characterization. *Remote Sens. Environ.* **2009**, *113*, S56–S66. [CrossRef]